Dissociation Kinetics between a Mouse Fc Receptor (FcγRII) and IgG: Measurement by Total Internal Reflection with Fluorescence Photobleaching Recovery†

Helen V. Hsieh‡ and Nancy L. Thompson*

Department of Chemistry, University of North Carolina, Chapel Hill, North Carolina 27599-3290

Received January 4, 1995; Revised Manuscript Received June 26, 1995®

ABSTRACT: Total internal reflection with fluorescence photobleaching recovery (TIR-FPR) has been used to examine the dissociation kinetics between monomeric mouse IgG and a mouse Fc receptor (moFcγRII) reconstituted into substrate-supported planar membranes. IgG1, IgG2a, and IgG2b exhibited similar dissociation kinetics, whereas IgG3 did not bind. The fluorescence recovery curves for the IgG−moFcγRII interactions were best described by two reversible components (1.4 s^{-1}, 66% and 0.06 s^{-1}, 18%) and an irreversible component (<0.01 s^{-1}, 16%). The kinetic parameters for a mouse anti-dinitrophenyl (DNP) IgG1 antibody were equivalent in the absence and presence of saturating amounts of DNP-glycine, demonstrating that possible allosteric changes which might occur in IgG1 upon hapten binding do not appreciably affect the kinetic characteristics of moFcγRII binding. The fluorescence recovery curves for polyclonal mouse IgG Fc were similar to those for intact IgG, showing that decreasing the size of the IgG 3-fold does not alter the dissociation rate. The dissociation kinetics of IgG1 decreased considerably in a low ionic strength buffer, indicating that the IgG1−moFcγRII interaction has significant electrostatic components.

The association of antibody−antigen complexes with immune cells triggers a diverse array of responses, including phagocytosis, antibody-dependent cell-mediated cytotoxicity, and B cell activation and regulation (Hulett & Hogarth, 1994; Ravetch & Kinet, 1991). These responses are initiated by the association of the Fc regions of antibodies and cell surface Fc receptors. The diversity of immune responses is generated in part by the heterogeneity of antibodies and their Fc receptors. Three Fc receptor isoforms for IgG (FcγRI, FcγRII, and FcγRIII) have been identified in mouse and human. The Fcγ receptor examined in this work is mouse FcγRII (moFcγRII)[1] (Mellman & Unkeless, 1980), which is a single-spanning transmembrane protein with two extracellular, glycosylated immunoglobulin-related domains.

The initiation of antibody-mediated cellular immune responses involves, in general, an interplay between chemical reaction processes (protein−protein interactions) and transport processes (lateral diffusion, rotational diffusion, and segmental flexibility both in solution and on the membrane). The manner in which these reaction and transport processes are coupled at the membrane surface is not yet clearly understood. The lack of physical information has been in part due to the heterogeneity of Fc receptors, the heterogeneity of antibodies, and the weak interactions between antibodies and some Fc receptors.

One method for obtaining quantitative, physical information about the coupled reaction and transport of proteins at membrane surfaces is to use substrate-supported planar membranes and techniques in fluorescence microscopy (Thompson et al., 1993a,b). In particular, illumination by total internal reflection may be combined with fluorescence photobleaching recovery (TIR-FPR) to examine the dissociation rates of proteins at supported planar membranes (Thompson et al., 1981; Burghardt & Axelrod, 1981). In this technique, the internal reflection of light generates a thin evanescent wave, which selectively excites fluorescent molecules bound to and near a surface. The dissociation of fluorescent molecules from the surface is investigated by using fluorescence photobleaching recovery, in which the fluorescence intensity preceding and following application of an intense pulse of light, which bleaches fluorescent molecules bound to the surface, is monitored as a function of time. TIR-FPR has recently been used to probe several biologically specific systems, including anti-dinitrophenyl (DNP) Fabs at planar membranes containing dinitrophenylated phospholipids (Pisarchick et al., 1992), prothrombin and its fragment 1 at planar membranes containing negatively charged phospholipids (Pearce et al., 1992, 1993), and epidermal growth factor at membranes containing its receptor (Hellen & Axelrod, 1991).

In previous work, mouse FcγRII (moFcγRII) was purified and reconstituted into substrate-supported planar membranes, and steady-state total internal reflection fluorescence microscopy was used to examine equilibrium aspects of IgG−moFcγRII reactions (Poglitsch et al., 1991; Hsieh et al., 1992). Here, TIR-FPR is used to examine the dissociation kinetics of IgG from the reconstituted moFcγRII.

† This work was supported by National Institutes of Health Grant GM-37145 (N.L.T.), National Science Foundation Grant GER-9024028 (N.L.T.), and a Department of Education Graduate Fellowship (H.V.H.).

* To whom correspondence should be addressed.

‡ Present address: Becton Dickinson Research Center, 21 Davis Drive, P.O. Box 12016, Research Triangle Park, NC 27709-2016.

® Abstract published in *Advance ACS Abstracts,* September 1, 1995.

[1] Abbreviations: BSA, bovine serum albumin; DMEM/F12, Dulbecco's modified Eagle's medium/Ham's F12; F-, fluorescein-labeled; DNP, dinitrophenyl; DNP-G, dinitrophenylglycine; FCS, fetal calf serum; HSA, human serum albumin; moFcγRII, mouse FcγRII; PB, phosphate buffer; PBS, phosphate-buffered saline; R-, tetramethylrhodamine-labeled; TIR-FPR, total internal reflection with fluorescence photobleaching recovery.

0006-2960/95/0434-12481$09.00/0

MATERIALS AND METHODS

Cells. J774A.1, a macrophage-like cell line containing cell surface moFcγRII, was obtained from the University of North Carolina Tissue Culture Facility. 2.4G2, a rat-mouse hybridoma which secretes antibodies specific for moFcγRII (Unkeless, 1979), was provided by B. Diamond of the Albert Einstein College of Medicine. DHK109.3 and DHK10.12, two mouse-mouse hybridomas which produce anti-DNP IgG1 and IgG2b, respectively (Liu et al., 1980), were obtained from N. R. Klinman and P. Linton, Scripps Clinic and Research Foundation. Cells were grown in DMEM/F12 media supplemented with 1 mM sodium pyruvate, 2 mM L-glutamine, 100 IU penicillin, 100 μg/mL streptomycin, and fetal calf serum (FCS) that had been heat inactivated for 30 min at 56 °C, as follows: J774A.1, 5% FCS; 2.4G2, 10% FCS; DHK109.3, 1% FCS, DHK10.12, 5% FCS. J774A.1 cells were also sometimes supplemented with 0.25 μg/mL amphotericin.

Antibodies. 2.4G2 antibodies were purified from cell supernatants by affinity chromatography with anti-(rat IgG κ light chain) antibodies, and 2.4G2 Fabs were produced and isolated as described (Poglitsch & Thompson, 1990). Intact mouse IgG2a, IgG3, and the Fc fragment of mouse IgG were obtained commercially (Jackson ImmunoResearch, Inc., West Grove, PA). DHK109.3 and DHK10.12 antibodies were purified from cell supernatants by affinity chromatography with DNP-conjugated human serum albumin (DNP-HSA) (Pisarchick & Thompson, 1990).

Antibodies were labeled with tetramethylrhodamine-5(and-6)-isothiocyanate or fluorescein isothiocyanate (Molecular Probes, Inc., Junction City, OR) as previously described (Timbs & Thompson, 1990) and dialyzed against phosphate-buffered saline (PBS; 0.05 M sodium phosphate, 0.15 M sodium chloride, 0.01% sodium azide, pH 7.4) or phosphate buffer (PB; 0.01 M sodium phosphate, 0.01% sodium azide, pH 7.4). The labeling ratios and antibody concentrations were determined spectrophotometrically. The molar ratio of fluorophore to antibody was $\approx$0.1 for each labeled antibody.

Labeled antibodies were clarified (100000*g*, 2 h, 4 °C) no more than 24 h prior to application to planar membranes. Gel filtration measurements (G200−120 Sephadex; 1.5 cm × 60 cm; flow rate, 0.03 mL/min; sample volume, 0.6 mL; PBS or PB; 25 °C) showed that F−Fc fragment and F-DHK109.3, R-DHK109.3, F-IgG2a, and F-DHK10.12 antibodies (0.1−1.0 mg/mL) eluted with symmetrical peaks corresponding to monomers. Possible higher molecular weight aggregates were not detected.

The immunoglobulin subclass of antibodies isolated from DHK109.3 supernatants was verified to be IgG1 with the EIA Grade Mouse Typer System (Bio-Rad Laboratories, Richmond, CA) (Sumner, 1993). This analysis also indicated that the commercial polyclonal mouse IgG consisted primarily of IgG1. The immunoglobulin subclass of antibodies isolated from DHK10.12 supernatants was verified to be IgG2b with the Sigma ImmunoType Mouse Monoclonal Antibody Isotyping Kit (Sigma Chemical Co., St. Louis, MO). This analysis also indicated that the commercial Fc fragment made from polyclonal mouse IgG consisted primarily of IgG2b.

Planar Membranes. MoFcγRII was purified from homogenized J774A.1 cells by 2.4G2 Fab affinity chromatography (Poglitsch et al., 1991; Mellman & Unkeless, 1980). The purity of the product was estimated with sodium dodecyl sulfate−polyacrylamide gel electrophoresis and silver staining. Previous N-terminal sequence determinations have confirmed that the purified product was moFcγRII (Poglitsch et al., 1991).

MoFcγRII was reconstituted into vesicles by detergent dialysis as described (Poglitsch et al., 1991), except that the lipid films were dried under vacuum for 4 h. The lipid composition was egg phosphatidylcholine/cholesterol (Sigma Chemical Co, St. Louis, MO) 6:1 (w:w), and the protein/lipid ratio was varied from 1:10 to 3:10 (w:w). Vesicles were also prepared without moFcγRII.

Membranes were formed on planar fused silica surfaces by vesicle adsorption and fusion as described (Hsieh et al., 1992). Planar membranes were treated with 10 mg/mL bovine serum albumin (BSA) in PBS (65 μL, 30 min) to block nonspecific binding sites and then treated with labeled antibodies in 10 mg/mL BSA/PBS (250 μL, 30 min). Some antibody solutions also contained 0.25 μM 2.4G2 Fab and/or 100 μM DNP-glycine (DNP-G).

Fluorescence Microscopy. The fluorescence microscope was composed of an argon ion laser (Innova 90-3, Coherent, Inc., Palo Alto, CA), an inverted optical microscope (Zeiss IM-35, Eastern Microscope Co., Raleigh, NC), and a single photon-counting photomultiplier (RCA C31034A, Lancaster, PA) interfaced to an IBM PC AT. TIR-FPR was carried out at room temperature as described (Pisarchick et al., 1992; Pearce et al., 1992), with the following parameters: laser wavelength, 488.0 or 514.5 nm; observation laser power, 5−200 μW; laser polarization, s-polarized or circularly polarized; incidence angle 75°; size of evanescent illumination area; 30 μm × 100 μm or 100 μm × 120 μm; objective (Zeiss), water, 40×, 0.75 N. A.; evanescent wave depth, $\approx$820 Å at 488.0 nm, $\approx$850 Å at 514.5 nm; bleach pulse laser power, 0.1−0.5 W; bleach pulse duration, 10−40 ms; bleach depth, 30−70%. For measurements with circularly polarized excitation light, a quarter-wave plate (Melles-Griot, Irving, CA) was introduced into the path of the laser beam. For each sample type and experimental parameter, measurements were obtained on planar membranes formed from at least two separate moFcγRII purifications. TIR-FPR recovery curves were fit to eq 1 with ASYST (Macmillan Software Co., New York).

RESULTS

Interaction of IgG with MoFcγRII in Substrate-Supported Planar Membranes. This paper describes characterization of the dissociation kinetics of monomeric mouse IgG at substrate-supported planar membranes containing purified and reconstituted moFcγRII. Supported planar membranes were formed by allowing detergent-dialyzed, receptor-containing phospholipid vesicles containing purified and reconstituted moFcγRII to adsorb and fuse at fused silica surfaces. A body of previous work suggests that this procedure results in continuous bilayers in which the lipids are well-oriented and undergo long-range lateral diffusion (Pearce et al., 1992; Gemmell et al., 1988; Zot et al., 1992). The reconstituted moFcγRII is not laterally mobile. In addition, approximately one-third of the receptors are accessible to binding by 2.4G2 Fab, and, of these, 25−50% bind mouse IgG (Poglitsch et al., 1991; Hsieh et al., 1992).

Specificity of IgG Binding to MoFcγRII in Planar Membranes. Previous measurements with steady-state total internal reflection fluorescence microscopy have shown that

IgG binds specifically to moFcγRII in planar membranes (Poglitsch et al., 1991). The equilibrium association constant was found to be $K = (3.6 \pm 0.5) \times 10^5\ M^{-1}$ (Hsieh et al., 1992). Binding specificity was demonstrated in that the evanescently excited fluorescence arising from labeled IgG on or near planar membranes was significantly reduced for membranes without moFcγRII, for labeled IgG Fab'$_2$, and in the presence of saturating amounts of 2.4G2 Fab. In the work described herein, two of these control samples, those without moFcγRII and those containing an excess (0.25 μM) of 2.4G2 Fab, were routinely monitored to confirm IgG−moFcγRII binding specificity.

Surface Binding Kinetics for IgG and MoFcγRII. TIR-FPR was used to investigate the surface binding kinetics of fluorescently labeled IgG with moFcγRII in planar membranes. The characteristic times for fluorescence recovery were on the order of several seconds, and recovery was nearly complete after 60 s (Figure 1a,b). The fluorescence intensity as a function of time was fit to a sum of exponentials

$$F(t) = F(-) - [a_0 + \sum_{i=1}^{n} a_i \exp(-\lambda_i t)] \quad (1)$$

where $F(-)$ was the prebleach fluorescence, and a_i (for $i = 0$ to n) and λ_i (for $i = 1$ to n) were free parameters. The fractional recoveries f_i and the bleached fractions β were calculated as

$$f_i = a_i[\sum_{i=0}^{n} a_i]^{-1} \quad (2)$$

$$\beta = [F(-)]^{-1} \sum_{i=0}^{n} a_i \quad (3)$$

The factors f_i are the fractions of the bleached fluorescence associated with rates λ_i, and f_0 is the fraction of the bleached fluorescence which does not recover within the time frame of the experiment. The TIR-FPR data were fit to monoexponential (Figure 1a; $n = 1$) and biexponential (Figure 1b; $n = 2$) forms of eq 1. The triexponential form ($n = 3$) of eq 1 contained too many free parameters for adequate fitting. Analysis with an F-statistic (Wright et al., 1988) indicated that the data for each IgG−moFcγRII interaction examined in this work were best described by two reversible components rather than one ($n = 2$). The best fit parameters for IgG−moFcγRII interactions were $f_0 = 0.16 \pm 0.03$, $\lambda_1 = 1.4 \pm 0.1\ s^{-1}$, $f_1 = 0.66 \pm 0.03$, $\lambda_2 = 0.06 \pm 0.01\ s^{-1}$, and $f_2 = 0.18 \pm 0.01$.

Controls for TIR-FPR Measurements. Several measurements were carried out to confirm that TIR-FPR data accurately report dissociation kinetics for IgG from moFcγRII in planar membranes (Table 1). The following data controlled for possible photoinduced artifacts during fluorescence photobleaching or monitoring: the fluorescence in the absence of photobleaching decreased ≤5% over the duration of fluorescence observation (60 s); the recovery curves were similar for two different fluorescence probes (fluorescein and tetramethylrhodamine); the recovery curves changed little with a 4-fold increase in the duration of the bleaching pulse or with a 5-fold increase in the intensity of the bleaching pulse; and the recovery curves were equivalent for repetitive bleaching on the same area (data not shown). Possible contributions to the fluorescence recovery that might arise from rotational motions were ruled out by confirming that the recovery curves did not change when the incident light was circularly, rather than linearly, polarized. Finally, little or no recovery was observed for fluorescein-labeled 2.4G2 Fabs (Figure 1c), which bind tightly ($K \approx 10^9\ M^{-1}$; Unkeless, 1979) to moFcγRII.

Reaction/Diffusion Effects in TIR-FPR. Previous theoretical work (Thompson et al., 1981; Hsieh & Thompson, 1994) has shown that TIR-FPR recovery curves depend in general on two types of characteristic rates: those that are functions only of the kinetic rate constants for a given surface binding mechanism, and those that describe transport. Within the second class of rates, there are three types: rates for diffusion in solution through a distance equal to the ratio of the surface density and the solution concentration (R), rates for diffusion in solution through the bleached area (R_L), and rates for diffusion along the surface through the bleached area (R_S).

The TIR-FPR recovery curves for IgG at planar membranes containing moFcγRII were equivalent within experimental error for bleached areas of different sizes (Table 1). Although contributions to fluorescence recovery that might arise from surface diffusion of IgG−moFcγRII complexes should be negligible in that the moFcγRII are not laterally mobile (Poglitsch et al., 1991), the lack of a dependence on the size of the bleached area indicates that, in addition, transport in solution in a direction parallel to the surface (R_S, R_L) does not appreciably contribute to the rate and shape of the fluorescence recovery curves. Therefore, the recovery curves may be analyzed by examining the theoretical forms for fluorescence recovery in limit of a large bleaching/observation area.

In the limit of a large area, TIR-FPR recovery curves depend only on the intrinsic kinetic rate constants and on the transport rates R (Thompson et al., 1981; Hsieh & Thompson, 1994). If the solution concentration is high and/or diffusion in solution is fast, contributions from R are minimal, and the TIR-FPR recovery curves are "reaction-limited". In this limit, bleached, dissociated molecules are rapidly replaced by unbleached molecules from solution, and the fluorescence recovery curves depend only on the intrinsic surface dissociation rate constants. If the solution concentration is low and/or diffusion in solution is slow, the TIR-FPR recovery curves are "diffusion-limited" and depend only on the transport rates R. As shown in Table 1, the TIR-FPR recovery curves for IgG−moFcγRII did not depend on the IgG concentration in solution. This result suggests that the data are in the reaction-limit. An additional condition for this limit is that the rate for transport in solution is much larger than the observed recovery rates. For a simple, reversible, bimolecular reaction, the transport rate is given by (Thompson et al., 1981)

$$R = \frac{D}{(KN)^2}(1 + KA)^2 \quad (4)$$

where D is the solution diffusion coefficient, A is the antibody solution concentration, and N is the density of surface-bound antibodies at saturation (see below). For $N = 300-1500$ molecules/μm^2, $D = 5 \times 10^{-7}$ cm^2/s, $K = 3.6 \times 10^5\ M^{-1}$, and $A = 1-10$ μM, R ranges from 120 to $3.3 \times 10^4\ s^{-1}$ and is therefore much greater than the observed rate of fluorescence recovery.

Effects of Antibody, Membrane, and Solution Characteristics on IgG−MoFcγRII Kinetics. The kinetic parameters

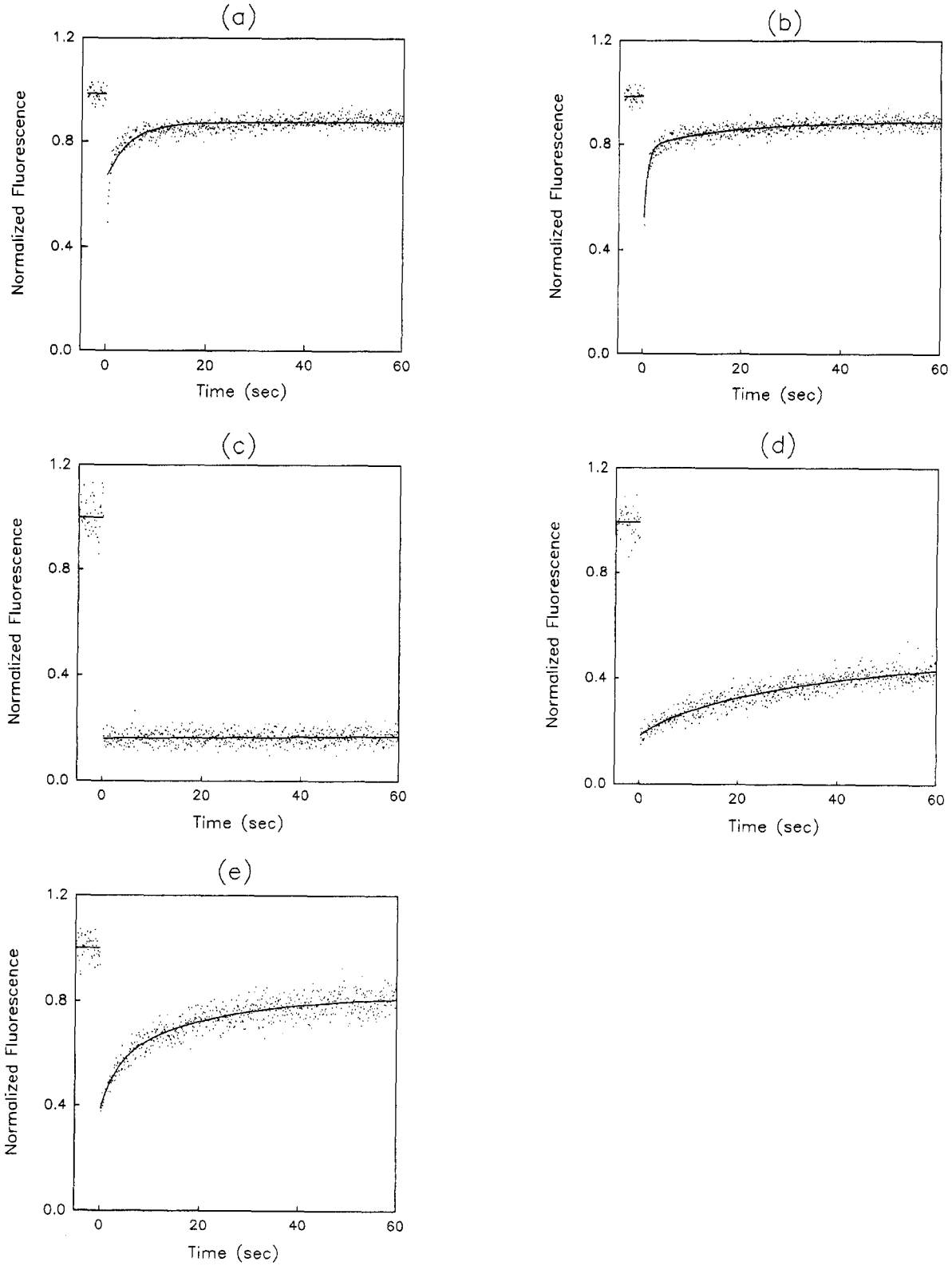

FIGURE 1: Typical TIR-FPR curves for fluorescently labeled IgG on planar membranes containing moFcγRII. The data are as follows: (a and b) 1 μM F-DHK109.3 in PBS; (c) 0.25 μM F-(2.4G2 Fab) in PBS; (d) 1 μM F-DHK109.3 with 4 μM DNP-HSA in PBS; and (e) 1 μM F-DHK109.3 in PB. The lines represent the best fits to (a) eq 1 with $n = 1$; (b, d, and e) eq 1 with $n = 2$; and (c) a line.

for IgG binding to moFcγRII with different antibody, membrane, and solution characteristics are shown in Table 2.

Several characteristics had no measurable effect on the kinetic rates and recoveries. The recovery curves for monoclonal IgG1 (DHK109.3), polyclonal IgG2a, and monoclonal IgG2b (DHK10.12) were similar (whereas IgG3 did not bind). A concentration of 100 μM DNP-G, which saturates nearly all of the antigen-binding sites of DHK109.3 (Hsieh et al., 1992) and causes only a small decrease in the fluorescence of the extrinsic probe (<20% for fluorescein; <5% for tetramethylrhodamine), had no measurable effect on the kinetic parameters.

Immune complexes were created by combining DNP-HSA and F-DHK109.3 (4:1, mol/mol; E. C. Bowles and N. L. Thompson, unpublished data). These immune complexes,

Table 1: Controls for TIR-FPR Measurements[a]

probe	bleaching power (W)	bleaching duration (ms)	polarization	[antibody] (μM)	observation area (μm × μm)	number of curves	λ_1 (s^{-1})	λ_2 (s^{-1})	f_1	f_2
F	0.5	10	linear(s)	1	30 × 100	13	1.3 ± 0.2	0.05 ± 0.01	0.60 ± 0.07	0.22 ± 0.04
F	0.5	40	linear(s)	1	30 × 100	15	1.2 ± 0.2	0.06 ± 0.01	0.59 ± 0.05	0.20 ± 0.02
F	0.1	40	linear(s)	1	30 × 100	15	1.6 ± 0.3	0.07 ± 0.03	0.64 ± 0.06	0.17 ± 0.03
R	0.5	10	linear(s)	1	30 × 100	13	1.6 ± 0.2	0.05 ± 0.02	0.73 ± 0.01	0.14 ± 0.01
F	0.5	10	linear(s)	1	100 × 120	14	1.5 ± 0.4	0.06 ± 0.05	0.68 ± 0.03	0.14 ± 0.02
F	0.5	10	linear(s)	10	30 × 100	10	1.6 ± 0.5	0.09 ± 0.05	0.76 ± 0.15	0.15 ± 0.03
F	0.5	10	circular	1	30 × 100	15	1.3 ± 0.3	0.06 ± 0.02	0.60 ± 0.05	0.22 ± 0.05
av							1.4 ± 0.1	0.06 ± 0.01	0.66 ± 0.03	0.18 ± 0.01

[a] Values were obtained from the best fits of TIR-FPR recovery curves to eq 1 with $n = 2$ and are the averages of 10−15 recovery curves. Uncertainties are standard deviations. For each sample type, data were obtained from at least two independent antibody and receptor preparations. Abbreviations are as follows: F, fluorescein-labeled; R, tetramethylrhodamine-labeled.

Table 2: Effects of Antibody, Membrane, and Solution Properties on IgG−MoFcγRII Kinetics[a]

antibody	solution	λ_1 (s^{-1})	λ_2 (s^{-1})	f_1	f_2
F-DHK109.3 (IgG1)	PBS	1.19 ± 0.18	0.06 ± 0.01	0.59 ± 0.05	0.20 ± 0.02
R-DHK109.3	PBS	1.59 ± 0.23	0.05 ± 0.02	0.73 ± 0.03	0.14 ± 0.04
F-polyclonal IgG2a	PBS	1.38 ± 0.52	0.07 ± 0.04	0.50 ± 0.07	0.20 ± 0.06
F-DHK10.12 (IgG2b)	PBS	1.15 ± 0.47	0.08 ± 0.03	0.40 ± 0.06	0.16 ± 0.02
F-polyclonal IgG Fc	PBS	1.18 ± 0.80	0.08 ± 0.04	0.43 ± 0.08	0.17 ± 0.03
F-DHK109.3	PBS, DNP-G	1.47 ± 0.25	0.05 ± 0.02	0.71 ± 0.05	0.21 ± 0.05
R-DHK109.3	PBS, DNP-G	1.59 ± 0.23	0.08 ± 0.06	0.71 ± 0.07	0.14 ± 0.04
F-DHK109.3	PB	0.35 ± 0.07	0.05 ± 0.02	0.39 ± 0.08	0.36 ± 0.04

[a] Values were obtained from the best fits of TIR-FPR recovery curves to eq 1 with $n = 2$ and are the averages of 3−15 recovery curves. Uncertainties are standard deviations. For each sample type, data were obtained from at least two independent antibody and receptor preparations. The antibody and DNP-G concentrations were 1 and 100 μM, respectively. The bleaching power and duration were 0.5 W and 10 or 40 ms. Abbreviations are as follows: DNP-G, DNP-glycine; F, fluorescein-labeled; PB, phosphate buffer; PBS, phosphate-buffered saline; R, tetramethylrhodamine-labeled.

which are multivalent in IgG and bind to moFcγRII more tightly than IgG monomers (Dower et al., 1981a), displayed a significantly higher irreversibly bound fraction and slower kinetic rates (Figure 1d). The best-fit parameters of the recovery curves for aggregates of F-DHK109.3, taken under similar conditions as curves for monomeric F-DHK109.3, exhibited a fast rate (0.35 s^{-1}, 11%), a slow rate (0.02 s^{-1}, 36%), and a fraction (53%) that was irreversible within the observation period (1 min). Recovery curves for F-DHK109.3 aggregates, observed for a longer period of time (13 min), exhibited a decreased fast rate (0.03 s^{-1}, 26%), a decreased slow rate (0.003 s^{-1}, 41%), and an irreversible fraction (33%).

Fluorescence recovery curves for F-DHK109.3 binding to moFcγRII were measured as a function of the density of reconstituted, IgG-binding moFcγRII. This density, N, was estimated by using

$$N \approx \frac{(r-1)dA}{\phi} \quad (5)$$

where r was the ratio of the fluorescence on membranes containing moFcγRII to the fluorescence on membranes without moFcγRII, d was the evanescent depth, and ϕ was the fraction of the surface sites that were saturated (Poglitsch et al., 1991). The best-fit parameters for recovery curves obtained on samples with moFcγRII densities ranging from 300 to 1500 molecules/μm^2 changed very little.

The rate of solute orientational diffusion has been predicted to have a strong effect on both kinetic association and dissociation rates in protein−protein and protein−membrane interactions. Therefore, TIR-FPR data were acquired for polyclonal mouse IgG Fc, which is approximately 3-fold smaller in size than intact IgG. As shown in Table 2, these measurements demonstrated no differences in the kinetic parameters for intact IgG and its Fc.

The kinetic parameters for F-DHK109.3 in a low ionic strength buffer (PB) were considerably different than those in the more physiological buffer, PBS. The fractional recovery and kinetic rate constant of the faster component decreased, and the fractional recovery of the slower rate increased (Figure 1e; Table 2).

DISCUSSION

IgG−MoFcγRII Kinetics—General Conclusions. TIR-FPR has been used to directly characterize the dissociation kinetics of monomeric mouse IgG at planar membranes containing purified and reconstituted moFcγRII. The fluorescence recovery curves changed little as control parameters were altered, indicating the absence of significant photoartifacts.

The TIR-FPR data were best described by two reversible components and a small irreversible component (1.4 s^{-1}, 66%; 0.06 s^{-1}, 18%; ≪0.06 s^{-1}, 16%). The slow rate agrees well with previous studies in which competitive radioimmunoassays were used to estimate the dissociation rate constant for monomeric IgG from cell surface Fc receptors (0.07 s^{-1}; Dower et al., 1981b; Hogg et al., 1987). The use of cell pelleting in the previous work limited the observable rate. In particular, a rate on the order of the fast rate measured in this paper with TIR-FPR would probably not have been observable.

The apparent association rate constants for DHK109.3 and moFcγRII, as calculated from the measured values of λ_1, λ_2, and the equilibrium association constant $K \approx 3.6 \times 10^5$ M^{-1}, were $\approx 5 \times 10^5$ and 2×10^4 M^{-1} s^{-1}. These values agree well with previously estimated kinetic association rate constants for mouse IgG−moFcγRII interactions (2×10^4 to 10^5 M^{-1} s^{-1}; Dower et al., 1981b; Hogg et al., 1987). Similarly slow association rate constants have been measured

by TIR-FPR in a number of biological model systems (Thompson et al., 1993a,b).

The kinetic association rates calculated from TIR-FPR data have differed from those measured in other studies in a particularly interesting manner. The association rate for an anti-DNP antibody binding to dinitrophenylated planar membranes was much lower than the rate for DNP-G in solution (Pisarchick et al., 1992), and the association rate for prothrombin fragment 1 binding to planar membranes was considerably lower than the rate for binding to small unilamellar vesicles (Pearce et al., 1992, 1993). However, the association rates for IgG and moFcγRII reconstituted into planar membranes, and for epidermal growth factor on cell membranes (Hellen & Axelrod, 1991), both agree with previous estimates on cell surfaces. This trend in TIR-FPR data suggests that the use of planar membranes may include features of the general mechanism of proteins binding to a surface (such as orientational, rebinding or electrostatic effects), which is omitted or different for molecules in solution or vesicles in suspension.

Heterogeneous Nature of IgG−MoFcγRII Dissociation Kinetics. The reaction-limited TIR-FPR recovery curves for IgG at planar membranes containing moFcγRII were not well described by a single exponential. Similar complex kinetic behavior has also been seen in other systems characterized with total internal reflection fluorescence microscopy, including bovine prothrombin fragment 1 at supported planar membranes containing phosphatidylserine (Pearce et al., 1992, 1993), anti-DNP Fabs at Langmuir−Blodgett films containing dinitrophenylated phosphatidylethanolamine (Pisarchick et al., 1992), fibrinogen at planar membranes containing reconstituted αIIbβ3 integrin (Müller et al., 1993), and epidermal growth factor on immobilized human epidermoid cells (Hellen & Axelrod, 1991). Nonmonoexponential kinetics have also been observed at cell surfaces, e.g., for IgE and antireceptor Fabs on mast cells containing moFcϵRI (Ortega et al., 1991) and for epidermal growth factor on human fibroblasts (Mayo et al., 1989).

There are a number of plausible explanations for the observed nonmonoexponential dissociation kinetics (Figure 2). Heterogeneity in the IgG (Figure 2a) might arise from different types of glycosylation (Nose & Wigzell, 1983; Leatherbarrow et al., 1985) or different binding sites on IgG for moFcγRII (Gergely & Sarmay, 1990; Diamond et al., 1985; Lund et al., 1992). Heterogeneity might also arise from the presence of a small population of IgG aggregates (see above); however, the absence of a significant amount of IgG aggregates was demonstrated by using gel filtration. This putative IgG heterogeneity is not likely to arise from the fluorescence labels in that the TIR-FPR recovery curves were equivalent for a range of independent labeling preparations using two different monoclonal antibodies (DHK109.3 and DHK10.12) and (for DHK109.3) two different fluorescence labels (fluorescein and tetramethylrhodamine isothiocyanate). The complex dissociation kinetics might also arise from heterogeneity in the moFcγRII (Figure 2b). Different moFcγRII types could plausibly result from different membrane orientations (Poglitsch et al., 1991), different binding sites on moFcγRII for IgG (Hogarth et al., 1992), or the presence of some receptor dimers. Nonspecific membrane binding has previously been demonstrated to be minimal in this system (Poglitsch et al., 1991; Hsieh et al., 1992).

The presence of more than one membrane-bound species would also result in nonmonoexponential TIR-FPR recovery curves. A mechanism in which IgG−moFcγRII complexes undergo an isomerization is consistent with the TIR-FPR data (Figure 2c). In addition, both the symmetric nature of IgG and the possibility of multiple binding IgG−moFcγRII contacts (Hogarth et al., 1992; Gergely & Sarmay, 1990; Diamond et al., 1985; Lund et al., 1992) suggest that IgG could bind to the membranes via sequential monovalent/bivalent attachment (Figure 2d). However, this latter mechanism is not consistent with the TIR-FPR data, in that they do not change substantially with the IgG solution concentration or the receptor density. In addition, a previous epifluorescence study (Poglitsch et al., 1991) of F-2.4G2 Fab on planar membranes containing reconstituted moFcγRII has shown that the receptors are uniformly distributed (within optical resolution) and do not undergo significant lateral diffusion. In that the highest receptor density used in the work described herein was 1500 molecules/μm^2, which corresponds to an average receptor−receptor distance of $\approx$250 Å, the likelihood that a significant number of the receptors are within close enough proximity so that one antibody could bind two receptors simultaneously, as required by the latter mechanism, is low.

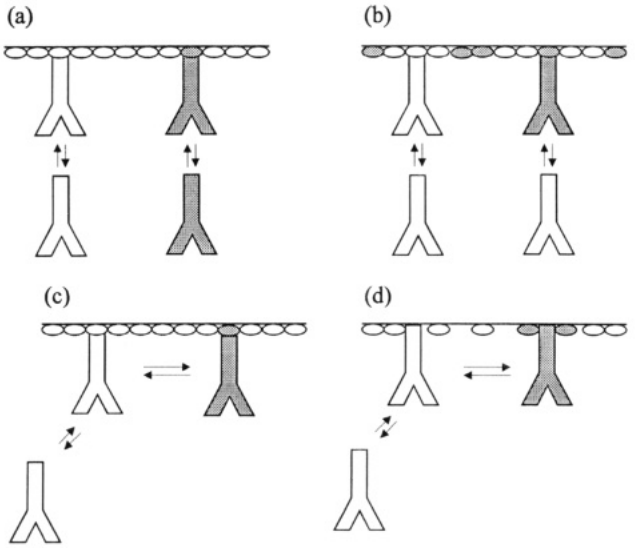

FIGURE 2: Mechanisms that result in biexponential TIR-FPR recovery curves: (a) two types of IgG in solution; (b) two types of moFcγRII binding sites on the membranes; (c) isomerization of the membrane-bound IgG−moFcγRII complexes; and (d) multiple membrane-bound states in which the IgG molecules may bind to one or two moFcγRII binding sites.

Protein−membrane interactions are often heterogeneous, as measured by a variety of methods and on a variety of systems (Pisarchick et al., 1992; Pearce et al., 1992, 1993; Hellen & Axelrod, 1991; Müller et al., 1993; Ortega et al., 1991; Mayo et al., 1989). There has also been recent theoretical activity addressing the complex nature of protein−membrane interactions [e.g., Steinbach et al. (1992), Nagle (1992), and Kopelman (1988)]. These experimental and theoretical studies suggest that the complex IgG−moFcγRII dissociation kinetics measured by TIR-FPR may arise from an intrinsic physical phenomena common to all protein−membrane interactions, such as crowding, rebinding, orientational, diffusional, or electrostatic effects.

Effect of IgG Subclass on Dissociation Kinetics. The observations that the IgG subclass specificities of different Fcγ receptors vary, that the expression of Fcγ receptors is cell-type specific, and that different effector functions are associated with different cell types (Ravetch & Kinet, 1991;

Unkeless et al., 1988; Mellman et al., 1988; Weinshank et al., 1988) suggest that the subclass specificity of Fcγ receptors is of physiological significance. For example, previous work has directly shown that some IgG-mediated immune responses can be subclass restricted for some categories of antigen (Perlmutter et al., 1978; Coutelier et al., 1991). Differences in the interactions of IgG subclasses with Fcγ receptors could presumably arise from differences in the amino acid sequences. The region of mouse IgG2b that binds moFcγRII is apparently in the C_H2 region (Diamond et al., 1985; Lund et al., 1992); and the C_H2 regions of IgG2a and IgG2b are 94% homologous to each other, but only 67% homologous to mouse IgG1 (Goding, 1986). Different receptor binding characteristics might also result from different glycosylations or segmental flexibilities (Oi et al., 1984; Dangl et al., 1988).

Early studies of Fcγ receptors in the mouse identified two receptors: moFcγRI, the high affinity, trypsin-sensitive IgG2a receptor, and moFcγRII, the low affinity, trypsin-resistant IgG1/2b Fcγ receptor (Walker, 1976; Unkeless, 1977; Heusser et al., 1977; Segal & Titus, 1978). However, later studies indicated that the low affinity IgG1/2b Fcγ receptor also weakly binds IgG2a (Mellman & Unkeless, 1980; Weinshank et al., 1988). The widespread presence of moFcγRII on different cell lines and variety of related functions has led to the suggestion that the specificity of moFcγRII for the different mouse IgG subclasses may vary with the cell type (Baum et al., 1985; Daëron et al., 1989). However, recent review articles have reached a consensus that moFcγRII weakly binds to monomeric IgG1, IgG2b, *and* IgG2a (Fridman, 1991; Ravetch & Kinet, 1991) and have suggested that the concurrent presence of moFcγRI on the same cells apparently masked the weaker IgG2a−moFcγRII association (Unkeless et al., 1988).

In this work, it has been shown that the kinetic parameters of moFcγRII are identical for monomeric mouse IgG1, IgG2a, and IgG2b (whereas IgG3 did not bind). This result is consistent with the previous work concluding that the equilibrium binding does not significantly differ for these IgG subclasses. The result does not provide a basis for postulating the physical basis that might underlay functional differences between these three IgG subclasses.

Saturation of the Hapten-Binding Site. The extent of conformational changes that may occur in antibodies upon binding haptens or antigens has not yet been fully resolved. Some structural studies for different antibodies have indicated that little if any conformational changes occur, whereas others have provided evidence for displacements in the variable and hypervariable regions or in the antigen (Poljak, 1975; Colman, 1988; Stanfield et al., 1990; Bhat et al., 1990; Davies et al., 1990; Wilson et al., 1991; Rini et al., 1992; Benjamin et al., 1992).

Functional studies have also produced conflicting results. For example, antigen was found to bind to IgE complexed with cell surface receptors with an affinity constant that is 4−11-fold higher than the one for antigen and IgE in solution (Kubitscheck et al., 1991). Because the interactions among antigen, antibody, and antibody receptor may be considered to be cyclic (Hsieh et al., 1992), this result suggests that IgE binds to cell-surface receptors more tightly when the antigen binding site is filled. In addition, antibody−antigen immune complexes have been found to bind more tightly to cell-surface Fcγ receptors than IgG oligomers of the same size (Leslie, 1985).

The kinetic parameters for the anti-DNP IgG1 antibody DHK109.3, with moFcγRII in planar membranes, were not measurably different in the presence or absence of saturating amounts of DNP-G. This result agrees with previous work examining the equilibrium binding constant of this antibody with moFcγRII (Hsieh et al., 1992; Sumner, 1993).

Molecular Size. Rotational diffusion has been predicted to be a major determinant in the kinetic association and dissociation rates of protein−protein and protein−membrane interactions (Baldo et al., 1991; Berg & von Hippel, 1985; Berg & Purcell, 1977; Schweitzer-Stenner et al., 1992). The effect of the size of the solution ligand on IgG−moFcγRII interactions was examined in this work by comparing the dissociation kinetics of monomeric IgG and IgG Fc. These measurement demonstrated no differences in the kinetic parameters for intact IgG and its Fc (molecular weight ratio, ≈3:1). Although earlier binding assays produced (conflicting) results suggesting significant differences between the binding of intact IgG and Fc to cell-surface Fc receptors (Dissanayake & Hay, 1975; Unkeless & Eisen, 1975), more recent functional studies, including measurements of sideways killing (Ito et al., 1989), platelet aggregation (Endresen, 1989), binding to virus-induced Fc receptors (Litwin et al., 1990), and prostaglandin synthesis (Suzuki, 1991), have not shown significant differences.

Effect of Ionic Strength. One of the earliest indications that more than one distinct class of human Fcγ receptors was present on monocyte cell lines was found by varying the ionic strength (Jones et al., 1985). Binding of aggregated mouse IgG2b was enhanced at low ionic strength, while binding of aggregated mouse IgG2a was unaffected. This difference in binding led to the identification of human FcγRII, which was later classified to be analogous to mouse FcγRII. A more recent study (Anderson et al., 1991) of FcγRII on human platelets also found that a decrease (3-fold) in ionic strength enhances the binding of immune complexes. The decrease in the IgG−moFcγRII dissociation rates measured by TIR-FPR, in a low salt buffer, is consistent with these previous results. The ionic strength dependence, which suggests that IgG−moFcγRII interactions involve a strong electrostatic component, is also consistent with results suggesting that a high fraction of the amino acids in FcγRII that participate in IgG binding are positively charged [E. C. Bowles and N. L. Thompson, unpublished data].

Summary. In this work, we have shown that TIR-FPR can be used to quantitatively examine the kinetics of weak interactions between protein ligands and receptors reconstituted into planar model membranes. The technique was used to characterize interaction of monomeric IgG with FcγRII for a range of membrane, antibody and solution characteristics. Possible future applications include characterization of the effects of extrinsic proteins such as complement components on the kinetics of IgG−FcγRII interactions, further investigations into the physical reasons for the observed heterogeneous kinetics, and extension of the method to other receptors that weakly bind protein ligands. In addition, when methods are developed for generating substrate-supported planar membranes that contain translationally mobile receptors, it may be possible to use TIR-FPR to quantitatively examine the kinetics of formation of IgG-induced receptor dimers.

ACKNOWLEDGMENT

We thank Betty Diamond of the Albert Einstein College of Medicine for providing 2.4G2 cells and Norman R. Klinman and Phyllis Linton of Scripps Clinic and Research Foundation for DHK109.3 and DHK10.12 cells. We also thank Diane Gesty-Palmer, Claudia L. Poglitsch and Martina T. Sumner for assistance with biological preparations.

REFERENCES

Anderson, G. P., van de Winkel, J. G. J., & Anderson, C. L. (1991) *Br. J. Haemotology 79*, 75−83.
Baldo, M., Grassi, A., & Raudino, A. (1991) *J. Phys. Chem. 95*, 6734−6740.
Baum, C. M., McKearn, J. P., Riblet, R., & Davie, J. M. (1985) *J. Exp. Med. 162*, 282−296.
Benjamin, D. C., Williams, D. C., Jr., Smith-Gill, S. J. S., & Rule, G. S. (1992) *Biochemistry 31*, 9539−9545.
Berg, H. C., & Purcell, E. M. (1977) *Biophys. J. 20*, 193−219.
Berg, O. G., & von Hippel, P. H. (1985) *Annu. Rev. Biophys. Biophys. Chem. 14*, 131−160.
Bhat, T. N., Bentley, G. A., Fischmann, T. O., Boulot, G., & Poljak, R. J. (1990) *Nature 347*, 483−485.
Burghardt, T. P., & Axelrod, D. (1981) *Biophys. J. 33*, 455−468.
Colman, P. M. (1988) *Adv. Immunol. 43*, 99−132.
Coutelier, J.-P., Van der Logt, J. T. M., & Heessen, F. W. A. (1991) *J. Immunol. 147*, 1383−1386.
Daëron, M., Sautès, C., Bonnerot, C., Blank, U., Varin, N., Even, J., Hogarth, P. M., & Fridman, W. H. (1989) *Chem. Immunol. 47*, 21−78.
Dangl, J. L., Wensel, T. G., Morrison, S. L., Stryer, L., Herzenberg, L. A., & Oi, V. T. (1988) *EMBO J. 7*, 1989−1994.
Davies, D. R., Padlan, E. A., & Sheriff, S. (1990) *Annu. Rev. Biochem. 59*, 439−473.
Diamond, B., Boccumini, L., & Birshtein, B. K. (1985) *J. Immunol. 134*, 1080−1083.
Dissanayake, S., & Hay, F. C. (1975) *Immunol. 29*, 1111−1118.
Dower, S. K., DeLisi, C., Titus, J. A., & Segal, D. M. (1981a) *Biochemistry 20*, 6326−6334.
Dower, S. K., Titus, J. A., DeLisi, C., & Segal D. M. (1981b) *Biochemistry 20*, 6335−6340.
Endresen, G. K. M. (1989) *Thromb. Res. 56*, 125−130.
Fridman, W. H. (1991) *FASEB J. 5*, 2684−2689.
Gemmell, C. H., Turitto, V. T., & Nemerson, Y. (1988) *Blood 72*, 1404−1406.
Gergely, J., & Sarmay, G. (1990) *FASEB J. 4*, 3275−3283.
Goding, J. W. (1986) *Monoclonal Antibodies: Principles and Practice*, Harcourt Brace Jovanovich, New York.
Hellen, E. H., & Axelrod, D. (1991) *J. Fluoresc. 1*, 113−128.
Heusser, C. H., Anderson, C. L., & Grey, H. M. (1977) *J. Exp. Med. 145*, 1316−1327.
Hogarth, P. M., Hulett, M. D., Ierino, F. L., Tate, B., Powell, M. S., & Brinkworth, R. I. (1992) *Immunol. Rev. 125*, 21−35.
Hogg, P. J., Reilly, P. E. B., & Winzor, D. J. (1987) *Biochemistry 26*, 1867−1873.
Hsieh, H. V., & Thompson, N. L. (1994) *Biophys. J. 66*, 898−911.
Hsieh, H. V., Poglitsch, C. L., & Thompson, N. L. (1992) *Biochemistry 31*, 11562−11566.
Hulett, M. D., & Hogarth, P. M. (1994) *Adv. Immunol. 57*, 1−127.
Ito, M., Usuba, O., Unkeless, J. C., Schreiber, R., Celada, F., Bona, C. A., & Moran, T. M. (1989) *Scand. J. Immunol. 29*, 659−669.
Jones, D. H., Looney, R. J., & Anderson, C. L. (1985) *J. Immunol. 135*, 3348−3353.
Kopelman, R. (1988) *Science 241*, 1620−1626.
Kubitscheck, U., Kircheis, M., Schweitzer-Stenner, R., Dreybrodt, W., Jovin, T. M., & Pecht, I. (1991) *Biophys. J. 60*, 307−318.
Leatherbarrow, R. J., Rademacher, T. W., Dwek, R. A., Woof, J. M., Clark, A., Burton, D. R., Richardson, N., & Feinstein, A. (1985) *Mol. Immunol. 22*, 407−415.
Leslie, R. G. Q. (1985) *Mol. Immunol. 22*, 513−519.
Litwin, V., Sandor, M., & Grose, C. (1990) *Virology 178*, 263−272.
Liu, F.-T., Bohn, J. W., Ferry, E. L., Yamamoto, H., Molinaro, C. Sherman, L. A., Klinman, N. R., & Katz, D. H. (1980) *J. Immunol. 124*, 2728−2737.
Lund, J., Pound, J. D., Jones, P. T., Duncan, A. R., Bentley, T., Goodall, M., Levine, B. A., Jefferis, R., & Winter, G. (1992) *Mol. Immunol. 29*, 53−59.
Mayo, K. H., Nunex, M., Burke, C., Starbuck, C., Lauffenburger, D., & Savage, C. R., Jr. (1989) *J. Biol. Chem. 264*, 17838−17844.
Mellman, I. S., & Unkeless, J. C. (1980) *J. Exp. Med. 152*, 1048−1069.
Mellman, I., Koch, T., Healey, G., Hunziker, W., Lewis, V., Plutner, H., Miettinen, H., Vaux, D., Moore, K., & Stuart, S. (1988) *J. Cell Sci. Suppl. 9*, 45−65.
Müller, B., Zerwes, H.-G., Tangemann, K., Peter, J., & Engel, J. (1993) *J. Biol. Chem. 268*, 6800−6808.
Nagle, J. F. (1992) *Biophys. J. 63*, 366−370.
Nose, M., & Wigzell, H. (1983) *Proc. Natl Acad. Sci. U.S.A. 80*, 6632−6636.
Oi, V. T., Vuong, T. M., Hardy, R., Reidler, J., Dangl, J., Herzenberg, L. A., & Stryer, L. (1984) *Nature 307*, 136−140.
Ortega, E., Schweitzer-Stenner, R., & Pecht, I. (1991) *Biochemistry 30*, 3473−3483.
Pearce, K. H., Hiskey, R. G., & Thompson, N. L. (1992) *Biochemistry 31*, 5983−5995.
Pearce, K. H., Hof, M., Lentz, B. R., & Thompson, N. L. (1993) *J. Biol. Chem. 268*, 22984−22991.
Perlmutter, R. M., Hansburg, D., Briles, D. E., Nicolotti, R. A., & Davie, J. M. (1978) *J. Immunol. 121*, 566−572.
Pisarchick, M. L., & Thompson, N. L. (1990) *Biophys. J. 58*, 1235−1249.
Pisarchick, M. L., Gesty, D., & Thompson, N. L. (1992) *Biophys. J. 63*, 215−223.
Poglitsch, C. L., & Thompson, N. L. (1990) *Biochemistry 29*, 248−254.
Poglitsch, C. L., Sumner, M. T., & Thompson, N. L. (1991) *Biochemistry 30*, 6662−6671.
Poljak, R. J. (1975) *Adv. Immunol. 21*, 1−33.
Ravetch, J. V., & Kinet, J.-P. (1991) *Annu. Rev. Immunol. 9*, 457−492.
Rini, J. M., Schulze-Gahmen, U., & Wilson, I. A. (1992) *Science 255*, 959−965.
Schweitzer-Stenner, R., Licht, A., & Pecht, I. (1992) *Biophys. J. 63*, 551−562.
Segal, D. M., & Titus, J. A. (1978) *J. Immunol. 120*, 1395−1403.
Stanfield, R. L., Fieser, T. M., Lerner, R. A., & Wilson, I. A. (1990) *Science 248*, 712−719.
Steinbach, P. J., Chu, K., Frauenfelder, H., Johnson, J. B., Lamb, D. C., Nienhaus, G. U., Sauke, T. B., & Young, R. D. (1992) *Biophys. J. 61*, 235−245.
Sumner, M. T. (1993) *FEBS Lett. 333*, 35−38.
Suzuki, T. (1991) *FASEB J. 5*, 187−193.
Thompson, N. L., Burghardt, T. P., & Axelrod, D. (1981) *Biophys. J. 33*, 435−454; and erratum, *Biophys. J. 35*, 809.
Thompson, N. L., Pearce, K. H., & Hsieh, H. V. (1993a) *Eur. Biophys. J. 22*, 367−378.
Thompson, N. L., Poglitsch, C. L., Timbs, M. M., & Pisarchick, M. L. (1993b) *Accts. Chem. Res. 26*, 567−573.
Timbs, M. M., & Thompson, N. L. (1990) *Biophys. J. 58*, 413−428.
Unkeless, J. C. (1977) *J. Exp. Med. 145*, 931−947.
Unkeless, J. C. (1979) *J. Exp. Med. 150*, 580−596.
Unkeless, J. C., & Eisen, H. N. (1975) *J. Exp. Med. 142*, 1520−1533.
Unkeless, J. C., Scigliano, E., & Freedman, V. H. (1988) *Annu. Rev. Immunol. 6*, 251−281.
Walker, W. S. (1976) *J. Immunol. 116*, 911−914.
Weinshank, R. L., Luster, A. D., & Ravetch, J. V. (1988) *J. Exp. Med. 167*, 1909−1925.
Wilson, I. A., Rini, J. M., Fremont, D. H., Fieser, G. G., & Stura, E. A. (1991) *Methods Enzymol. 203*, 153−176.
Wright, L. L., Palmer, A. G., III, & Thompson, N. L. (1988) *Biophys. J. 54*, 463−470.

BI9500180